**Supporting Information**

# Construction of Hierarchical ZnIn$_2$S$_4$/C$_3$N$_4$ Heterojunction for Enhanced Photocatalytic Degradation of Tetracycline

Feng Min[1]; Zhengqing Wei[1]; Yuting Xiao[1]*; Shien Guo[2]; Renjie Song[1]*; Jinheng Li[1,3]*

1. Key Laboratory of Jiangxi Province for Persistent Pollutants Control and Resources Recycle, Nanchang Hangkong University, Nanchang 330063, China

2. Institute of Advanced Materials (IAM), College of Chemistry and Chemical Engineering, Jiangxi Normal University, Nanchang 330022, People's Republic of China

3. School of Chemistry and Chemical Engineering, Henan Normal University, Xinxiang, Henan 475004, China

# Experimental section

## Materials

All of the reagents were received from Aladdin industrial Inc. and used without further purification.

## Synthesis of tubular $C_3N_4$ (TCN)

As reported in previous literature [1], firstly, 1 g melamine and 1.2 g phosphorous acid were dissolved in 100 ml deionized water at 80°C in constant temperature oil-bath pans with strong stirring for 1h. Then the solution was transferred into an autoclave with Teflon liner and heated at 180 °C for 10 hours. The mixture was centrifuged, washed with deionized water and ethanol for several times until the phosphorus species were removed out. Finally, the supramolecular precursors were obtained after drying at 60 °C in the oven. The appropriate amount of precursor was uniformly distributed in porcelain boat and placed in a muffle furnace, heated to 550 °C with rate of 2 °C/min and kept for 4 hours, the resultant sample was denoted as TCN.

## Preparation of ZIS/TCN composites

In detail, 100 mg TCN was dispersed into a mixed alcoholic solution that contained glycerol (5 mL) and ethanol (15 mL). Then, certain amount of $Zn(CH_3COO)_2$, $In(NO_3)_3$ and $C_3H_7NO_2S•HCl$ was added into the above solution under stirring one by one, followed by stirring for another several minutes. Finally, the obtained yellow solution was transferred to a 50 mL Teflon-lined stainless steel autoclave, which was heated to 180 °C and maintained for 12 h. After cooling, the as-synthesized brown products were rinsed three times with ethanol and dried at 60 °C overnight. The obtained product named as ZIS-CN-x (x=1, 2, 3, 4, which represents the mass ratio of ZIS to TCN).

## Preparation of $ZnIn_2S_4$ (ZIS)

For comparison, pure $ZnIn_2S_4$ was prepared using the same solvothermal method without the addition of $C_3N_4$ tube.

# Characterizations

The crystal phases of the photocatalysts were analyzed by powder X-ray diffraction (Bruker, Billerica, MA, USA) with Cu K (k = 0.15418 nm) radiation with scanning angle ranged from 5 to 80°. The morphological of all the photocatalysts samples were observed by scanning electron microscopy (Hitachi S-4800) and transmission electron microscopy (JEOL-2100F). Fourier transform infrared (FT-IR) spectra were collected on a Nicolet IS5 FT-IR spectrophotometer. The surface chemical compositions of the pre-prepared samples were performed by X-ray photoelectron spectra (XPS, Thermo ESCALAB250, Thermo Scientific, USA). Photoluminescence (PL) spectra were measured by Hitachi F-7000 fluorescence spectrophotometer. UV–vis diffuse reflection spectra (DRS) were recorded using Lambda750 S with $BaSO_4$ as reference. The time-resolved fluorescence (TRPL) decay spectra were measured by FS5 spectrofluorometer. UV–vis adsorption spectroscopy was taken on a Metash UV-9000S UV–vis spectrometer. Brunauer–Emmett–Teller (BET) specific surface area of the samples was obtained on a Belsorp-Mini II analyzer (Japan). High performance liquid mass spectrometry data of all the products were collected by Waters Xevo G2 QTof (Q-TOF/IT-TOF, USA). Total organic carbon was measured using an Elementar vario TOC analyzer.

**Photocatalytic degradation performance test**

Typically, 10 mg of as-prepared photocatalyst was dispersed in 60 mL of pollutant aqueous solution (rhodamine B, Methylene blue and tetracycline, 20 mg/L). Prior to visible light irradiation, the suspension was magnetically stirred for 10 min in the dark to ensure the establishment of an adsorption–desorption equilibrium between the photocatalysts and pollutions. A 300 W Xenon lamp (CEL-HXF300) equipped with UV-cut 400 nm filter was used as the visible light source. At regular irradiation time intervals, aliquots (5 mL) were sampled and centrifuged to separate the suspended catalysts. The concentration of residual pollutants was detected by a UV–vis absorption spectrometer (UV-9000S) spectrophotometer at their characteristic absorption wavelength. The degradation efficiency ($\eta$) and the apparent rate constant ($k_{app}$) can be calculated by following formulas:

$$\eta = \frac{C - C_0}{C_0} \times 100\%$$

(1)

$$\ln\frac{C_0}{C} = k_{app}t$$

(2)

where: $C_0$ represents the initial concentration of contaminant solution, C is the measured absorbance of contaminant solution after the reaction, and t is the reaction time.

## Photoelectrochemical measurements

The photocurrent measurements were measured by electrochemical workstation (CHI 660D, Shanghai) with a conventional three-electrode system under visible light illumination. Fluorine-doped tin oxide (FTO) conductive glass dip coated with the samples were viewed as the working electrode, a Pt electrode was treated as the assistance electrode, Ag/AgCl electrode was employed as the reference electrode, and 0.2 M $Na_2SO_4$ was used as electrolyte solution. Nyquist plots were validated by an amplitude perturbation of 0.2 V with the frequency range of 100 kHz to 0.1 Hz under the open circuit potential. Mott-Schottky plots were determined in 0.2 M $Na_2SO_4$ at various frequencies.

## Capturing experiment

Sacrificial agents such as isopropanol (IPA, 1mM), disodium ethylenediaminetetraacetate (EDTA-2Na, 1 mM), 1,4-benzoquinone (BQ, 1 mM) and argon (Ar) were used to probe hydroxyl radicals (•OH), holes ($h^+$), superoxide radicals (•$O_2^-$) and $O_2$ respectively during the photocatalytic degradation of pollutants. In these experiments, 10 mg ZIS/TCN-3 was added to 60 mL of contaminant aqueous solution (20 mg $L^{-1}$), followed by the addition of scavenging agent, and the mixture was illuminated for the degradation of target pollutant.
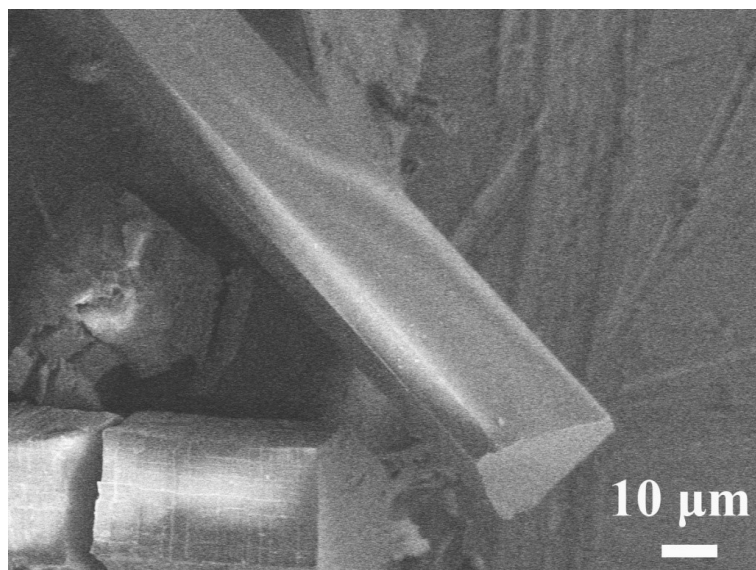
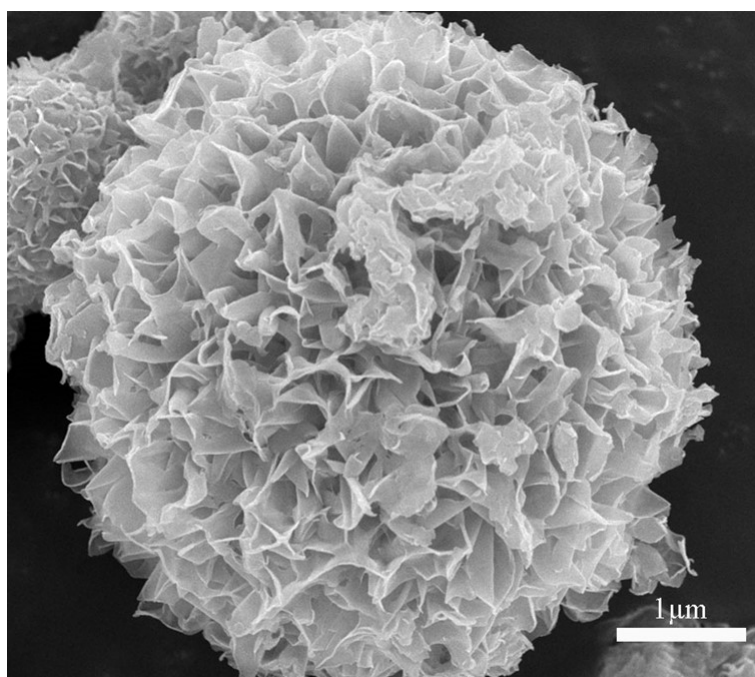**Figure S1.** Scanning electron microscope image of supramolecular precursors.



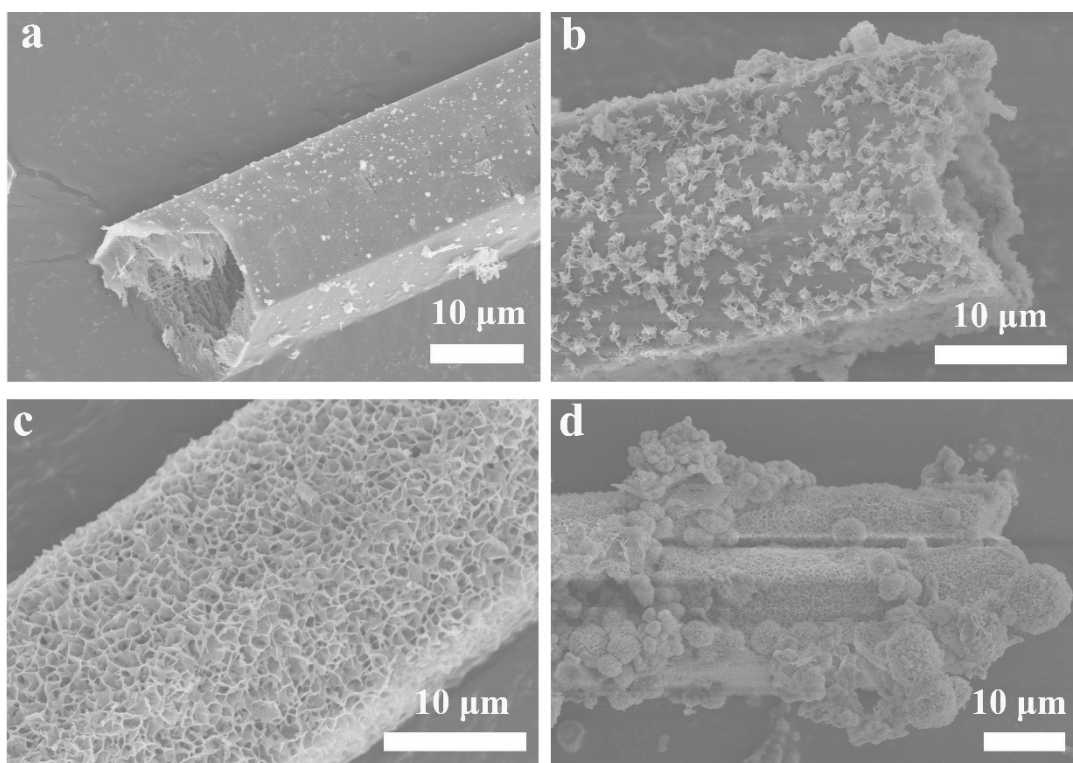**Figure S2.** Scanning electron microscope image of ZIS

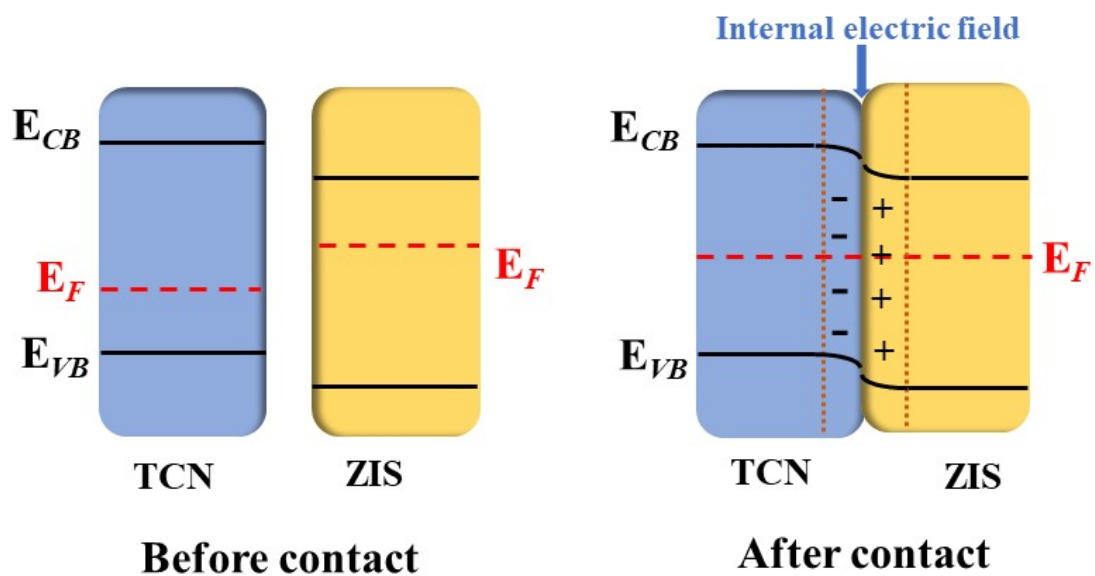**Figure S3.** SEM images of the different samples: a. ZIS/TCN-1, b. ZIS/TCN-2, c. ZIS/TCN-3, d. 50%- ZIS/TCN-4.



**Figure S4.** Schematic diagram of the spatial dynamic behavior of the charges across the interface of TCN and ZIS.
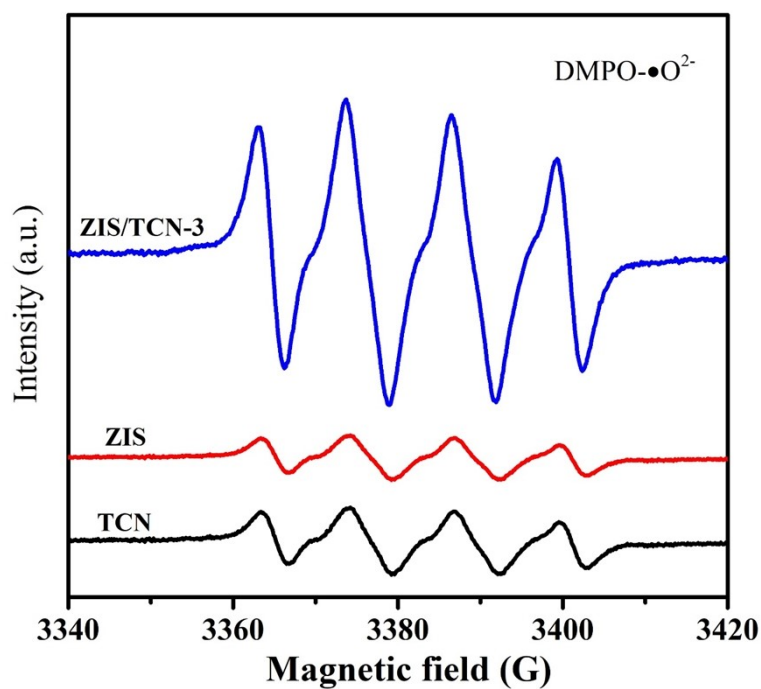
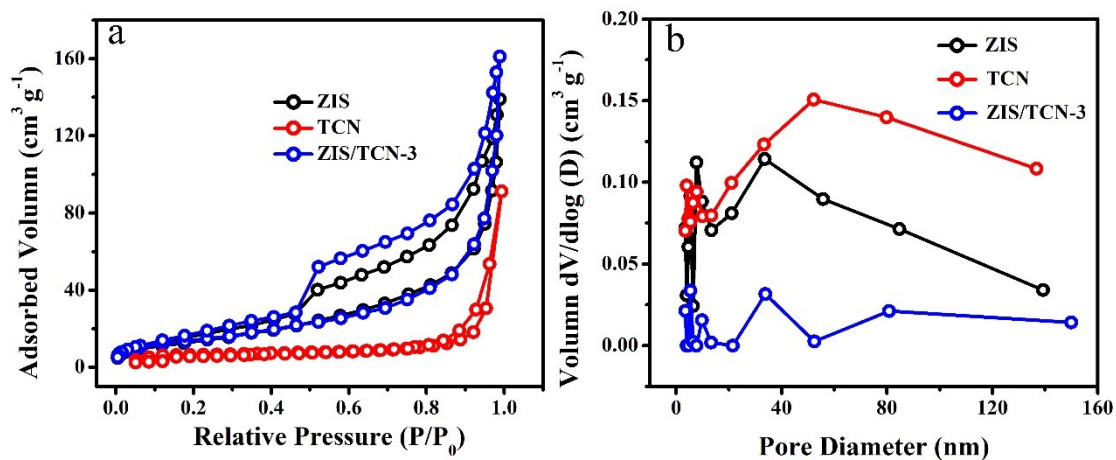**Figure S5**. ESR spectra of TCN, ZIS and ZIS/TCN recorded for DMPO-•$O^{2-}$.



**Fig. S6.** $N_2$ sorption isotherms of ZIS, TCN and ZIS/TCN-3 with the inset displaying the corresponding pore size distribution curves.

**Table S1.** Barrett-Joyner-Halenda (BJH) specific area and pore volume of different samples.

| Photocatalysts | $S_{BET}$ (m$^2$ g$^{-1}$) | Pore Volume (cm$^3$ g$^{-1}$) |
| --- | --- | --- |
| ZIS | 43.9 | 0.12 |
| TCN | 21.6 | 0.15 |
| ZIS/TCN-3 | 50.7 | 0.24 |

**Table S2.** Fitted parameters from time-resolved PL spectra of pristine ZIS, TCN and ZIS/CN-3.

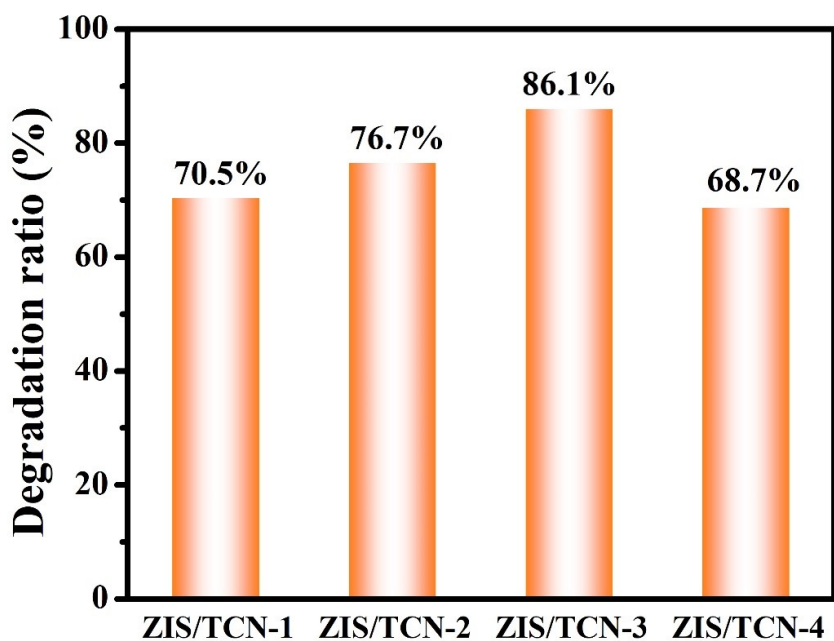| Photocatalysts | $\tau_1$ | $B_1$ | $\tau_2$ | $B_2$ | $\tau$ |
| --- | --- | --- | --- | --- | --- |
| ZIS | 1.1209 | 0.066 | 5.5463 | 0.009 | 2.90 |
| TCN | 0.4125 | 0.123 | 3.9337 | 0.009 | 1.86 |
| ZIS/TCN-3 | 1.4335 | 0.054 | 7.6442 | 0.012 | 4.80 |

**Figure S7.** Photodegradation rate of tetracycline on different samples under visible light.
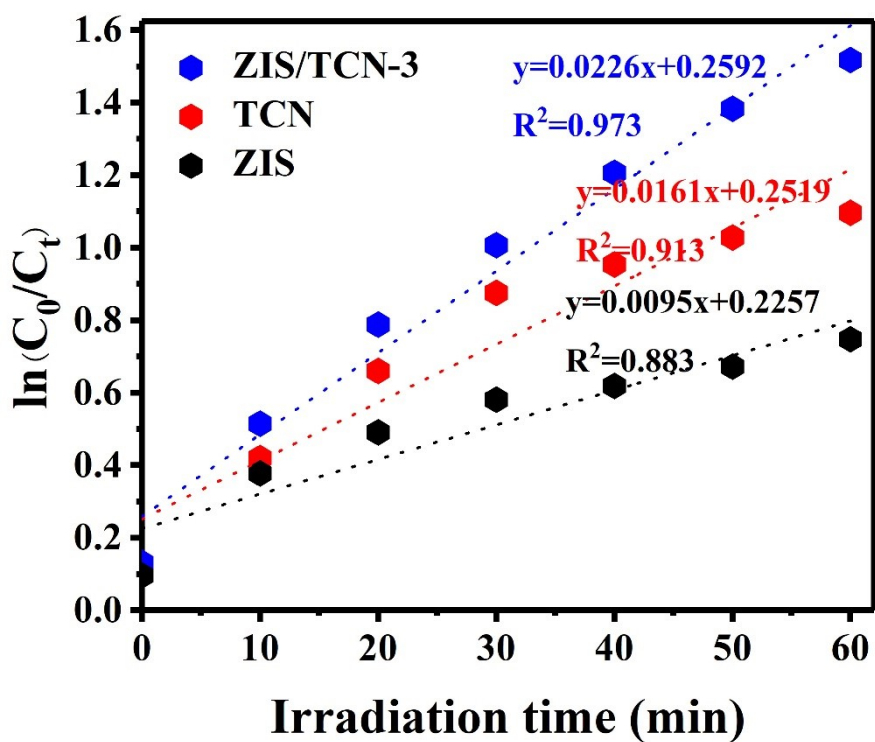


**Figure S8.** The corresponding kinetic analysis with the photocatalytic degradation performances of tetracycline on different samples under visible light.

**Table S3**. The comparison of TC decomposition by ZIS/TCN-3 with $C_3N_4$-based catalyst

| Photocatalyst | Light source | Catalyst weight (mg) | $C_{TC}(mg \cdot L^{-1})$ | Rate constant | Reference |
|---|---|---|---|---|---|
| Ag/g-$C_3N_4$ | 300W, Xe lamp ($\lambda > 420$ nm) | 50 | 20 | 0.0120 min$^{-1}$ | [2] |
| $\alpha$-$Fe_2O_3$/d-$C_3N_4$ | 500W, Xe lamp ($\lambda > 420$ nm) | 20 | 20 | 0.0103 min$^{-1}$ | [3] |
| BiOI/g-$C_3N_4$/ CeO$_2$ | 300W, Xe lamp ($\lambda > 420$ nm) | 50 | 20 | 0.0205min$^{-1}$ | [4] |
| Cl-doped g-$C_3N_4$ | 300W, Xe lamp ($\lambda > 420$ nm) | 50 | 10 | 0.0201min$^{-1}$ | [5] |
| $ZnSnO_3$/g-$C_3N_4$ | 300W, Xe lamp ($\lambda > 420$ nm) | 25 | 10 | 0.0131 min$^{-1}$ | [6] |
| $WO_3$/g-$C_3N_4$ | 300W, Xe lamp ($\lambda > 420$ nm) | 100 | 10 | 0.0213min$^{-1}$ | [7] |
| $TiO_2$/HCCN | 300W, Xe lamp ($\lambda > 420$ nm) | 50 | 10 | 0.0203 min$^{-1}$ | [8] |
| $LaNiO_3$/g-$C_3N_4$ | 300W, Xe lamp ($\lambda > 420$ nm) | 50 | 20 | 0.0028 min$^{-1}$ | [9] |
| $LaMnO_3$/g-$C_3N_4$ | 300W, Xe lamp ($\lambda > 420$ nm) | 50 | 20 | 0.0080 min$^{-1}$ | [10] |
| $\alpha$-$Bi_2O_3$/g-$C_3N_4$ | 300W, Xe lamp ($\lambda > 400$ nm) | 50 | 10 | 0.0122min$^{-1}$ | [11] |
| ZIS/TCN-3 | 300W, Xe lamp ($\lambda > 400$ nm) | 10 | 20 | 0.0226 min$^{-1}$ | This work |
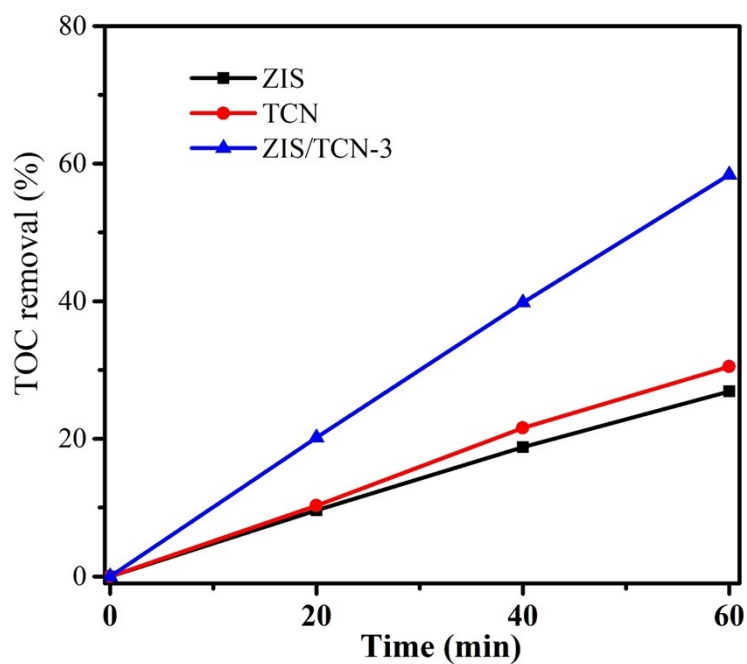
**Figure S9**. Total Organic Carbon (TOC) removal of the different samples during photocatalytic degradation process.



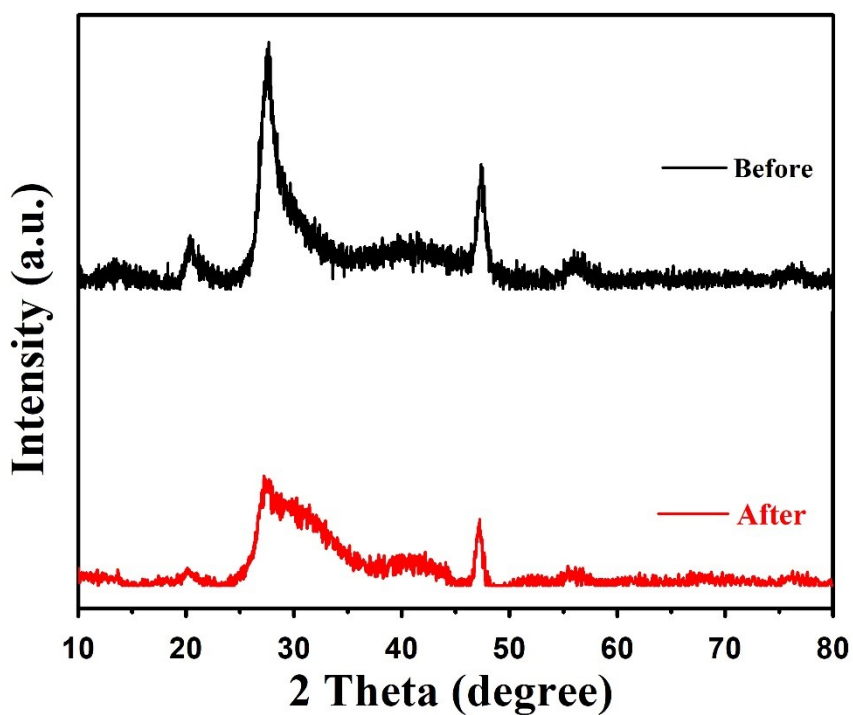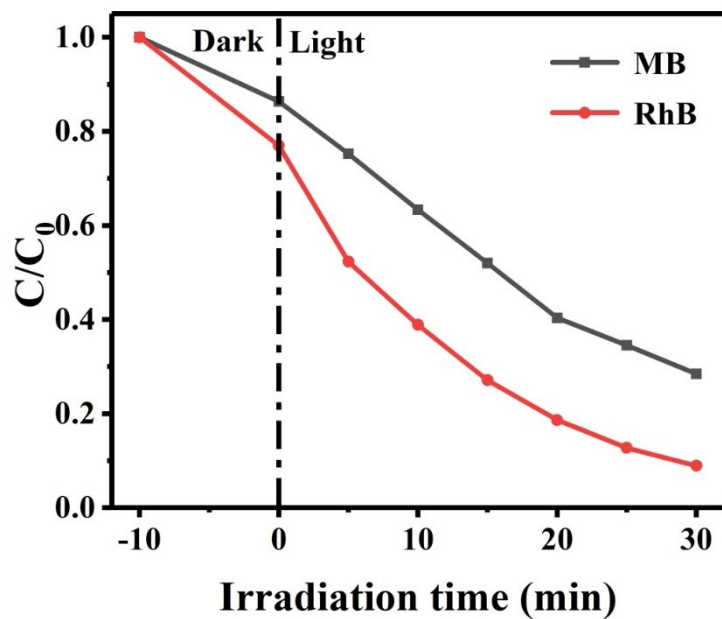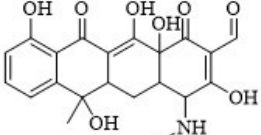**Figure S10.** XRD pattern of fresh and used ZIS/CN-3 after five cycles.
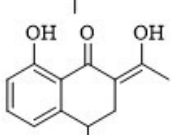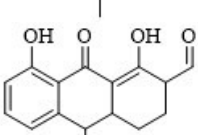
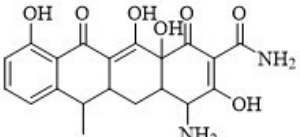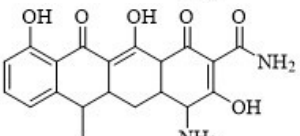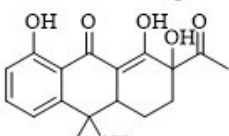**Fig. S11.** Photocatalytic degradation of RhB and MB with the as-prepared ZIS/CN-3 heterojunctions as photocatalysts under visible light.
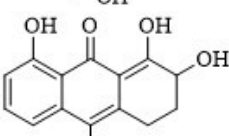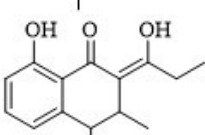
**Table S4**. Mass spectrometry information and proposed structures of the photocatalytic products of tetracycline.

| Number | Retention Time/min | m/z | Supposed Structure |
|--------|--------------------|-----|--------------------|
| tetracycline | 1.93 | 445 |  |
| 1 | 1.93 | 429 |  |
| 2 | 1.93 | 445 |  |
| 3 | 2.10 | 459 |  |

| | | | |
|---|---|---|---|
| 4 | 2.73 | 416 |  |
| 5 | 3.00 | 401 |  |
| 6 | 1.93 | 385 |  |
| 7 | 4.36 | 318 |  |
| 8 | 6.77 | 258 |  |
| 9 | 3.57 | 246 |  |
| 10 | 2.73 | 218 |  |
| 11 | 4.33 | 274 |  |

REFERENCES

1.      Xiao, Y., et al., *Molecule Self-Assembly Synthesis of Porous Few-Layer Carbon Nitride for Highly Efficient Photoredox Catalysis.* J Am Chem Soc, 2019. **141**(6): p. 2508-2515.

2.      Xu, W., et al., *Visible light photocatalytic degradation of tetracycline with porous Ag/graphite carbon nitride plasmonic composite: Degradation pathways and mechanism.* J Colloid Interface Sci, 2020. **574**: p. 110-121.

3.      Wang, S., et al., *Defect as the essential factor in engineering carbon-nitride-based visible-light-driven Z-scheme photocatalyst.* Applied Catalysis B: Environmental, 2020. **260**: p. 118145.

4.      Jiang, X., et al., *Novel ternary BiOI/g-C$_3$N$_4$/CeO$_2$ catalysts for enhanced photocatalytic degradation of tetracycline under visible-light radiation via double charge transfer process.* Journal of Alloys and Compounds, 2019. **809**: p. 151804.

5.      Guo, F., et al., *Facile bottom-up preparation of Cl-doped porous g-C$_3$N$_4$ nanosheets for enhanced photocatalytic degradation of tetracycline under visible light.* Separation and Purification Technology, 2019. **228**: p. 115770.

6.      Huang, X., et al., *Hydrothermal synthesis of ZnSnO$_3$ nanoparticles decorated on g-C$_3$N$_4$ nanosheets for accelerated photocatalytic degradation of tetracycline under the visible-light irradiation.* Separation and Purification Technology, 2020. **230**: p. 115854.

7.      Yan, H., et al., *Single-source-precursor-assisted synthesis of porous WO$_3$/g-C$_3$N$_4$ with enhanced photocatalytic property.* Colloids and Surfaces A: Physicochemical and Engineering Aspects, 2019. **582**: p. 123857.

8.      Guo, F., et al., *Fabrication of TiO$_2$/high-crystalline g-C$_3$N$_4$ composite with enhanced visible-light photocatalytic performance for tetracycline degradation.* Journal of Chemical Technology & Biotechnology, 2020.

9.      Zhou, X., et al., *Construction of LaNiO$_3$ nanoparticles modified g-C$_3$N$_4$ nanosheets for enhancing visible light photocatalytic activity towards tetracycline degradation.* Separation and Purification Technology, 2019. **211**: p. 179-188.

10.     Luo, J., et al., *Rational construction of direct Z-scheme LaMnO$_3$/g-C$_3$N$_4$ hybrid for improved visible-light photocatalytic tetracycline degradation.* Separation and Purification Technology, 2019. **211**: p. 882-894.

11.     Chen, D., et al., *A nanosheet-like α-Bi$_2$O$_3$/g-C$_3$N$_4$ heterostructure modified by plasmonic metallic Bi and oxygen vacancies with high photodegradation activity of organic pollutants.* Separation and Purification Technology, 2018. **193**: p. 232-241.